Acta Cryst. (1972). B28, 1899

Structure and Thermal Expansion of Beryl*

BY B. MOROSIN

Sandia Laboratories, Albuquerque, New Mexico 87115, *U.S.A.*

(*Received* 8 *September* 1971)

The crystal structure of beryl, $Al_2Be_3(SiO_3)_6$, has been refined by the least-squares analysis of 1981 counter-measured Mo $K\alpha$ intensities. Positional parameters are in excellent agreement, and anisotropic thermal parameters are compared with isotropic values recently obtained by Gibbs, Breck & Meagher, *Lithos* (1968) **1**, 275. Lattice constants, as a function of temperature, have been determined over the temperature range +25 to 800°C for beryl and −200 to 800°C for emerald (chrome doped beryl). At room temperature, the thermal expansivities of beryl are $+(2{\cdot}6\pm0{\cdot}1)\times10^{-6}°C^{-1}$ and $-(2{\cdot}9\pm0{\cdot}4)\times10^{-6}°C^{-1}$ along the *a* and *c* axes, respectively, while for emerald, the corresponding values are $+(1{\cdot}7\pm0{\cdot}1)\times10^{-6}°C^{-1}$ and $\sim(0{\cdot}16\pm0{\cdot}6)\times10^{-6}°C^{-1}$. However, a meaningful comparison of the thermal expansion behavior of the two materials can be made only by considering a large temperature interval rather than any particular temperature.

Introduction

Recently, we have been studying several oxide materials that exhibit anisotropic thermal expansion (Morosin & Lynch, 1971). Cartz (1968) and Li & Peacor (1968) have suggested that the critical feature of crystalline anisotropy, leading to thermal expansion anisotropy, is the degree of distortion of the atomic coordination polyhedra, *i.e.*, how markedly the bond lengths and angles vary about cations. Therefore, we considered beryl, because of its thermal expansion behavior (expansion along the *a* axis and contraction along the *c* axis with increasing temperature: *Handbook of Chemistry and Physics*, 1957), and because its structural unit consists of irregular tetrahedra (Si–O distances varying from 1·54 to 1·68 Å; Belov & Matveeva, 1951).

Our room-temperature structural study on beryl was completed before we became aware of the work of Gibbs, Breck & Meagher (1968; hereafter, GBM). These authors had determined and compared the crystal structures of beryl and emerald (chrome doped beryl), which had been grown by hydrothermal and molten-flux methods at the Linde Laboratories. Their results established the location of the water in the lattice for hydrothermally grown crystals and also showed that the previously observed differences in the Si–O distances existed; however, these differences were not as large as those reported by Belov & Matveeva (1951). Our positional parameters are in excellent agreement with GBM's study; therefore, in this paper we compare their isotropic thermal parameters with our anisotropic values obtained from a larger number of intensity data and report the lattice constants as a function of temperature for beryl.

* This work was supported by the U. S. Atomic Energy Commission.

Experimental

Gem-quality crystals of beryl and emerald, which were cut as cubes ~0·03 cm on edge, were obtained from Wolff Engineering Corporation, Newport Beach, California. Spectroscopic analysis of the beryl material indicated about 0·1 wt.% Fe and trace (≤0·001%) amounts of K and Ca; the analysis of emerald indicated about 0·3 wt.% Cr, about 0·05 wt.% Fe, and trace amounts of Mg, Ca, and Ti.

Precession photographs showed systematic absences for reflections of the type *hhl* and *h*0*l* for *l* odd, which were consistent with the previously assigned (Bragg & West, 1926; confirmed by Belov & Matveeva (1951) as well as GBM) space group of $P6/mcc$. Lattice constants, at room temperature, of $a_o=9{\cdot}2088$ (5) and $c_o=9{\cdot}1896$ (7) Å were determined by least-squares analysis of 12 high 2θ reflections measured on films taken with a 115 mm diameter Weissenberg camera, utilizing Straumanis film loading and Cu $K\alpha$ radiation (λ for $K\alpha_1=1{\cdot}54050$ Å). There are two formula units of $Be_3Al_2(SiO_3)_6$ in a unit cell, yielding a calculated density of 2·66 g.cm^{-3}.

Three symmetry-equivalent sets of Mo $K\alpha$ intensity data ($2\theta\leq130°$) were measured with a scintillation counter, employing pulse-height discrimination. The θ–2θ scan technique was employed using a speed of $\frac{1}{2}°$ min^{-1} over the interval $2\theta_{\lambda2}-1{\cdot}25°$ to $2\theta_{\lambda2}+1{\cdot}25°$ with 20 sec background counts, each at the beginning and end of the scan. These data yielded 1981 unique *hkl* reflections, of which 251 were measured to be less than 3σ [$\sigma=(n_{sc}+k^2n_b)^{1/2}$, where n_{sc}, n_b, and k are the total scan count, background counts, and ratio of the scan-to-background-time, respectively]; hence, they were assigned a value equal to 3σ and were considered to be unobserved in subsequent calculations. Absorption corrections were not considered necessary

($\mu = 8{\cdot}56$ cm^{-1}) for the crystal specimen (0·26 mm cube mounted on [11$\bar{2}$0]) used.

Lattice constants, as a function of temperature, were measured using a high-temperature single-crystal furnace described elsewhere (Lynch & Morosin, 1971). In general, 8 to 12 different 2θ values (between 115 to 160° 2θ) were measured on a Picker diffractometer and were reduced, by least-squares analysis, to specific values for the a and c axes. When it was discovered that the thermal expansivities for beryl differed from those given in the *Handbook of Chemistry and Physics* (1957), an emerald crystal was studied to evaluate the effect of impurities on the thermal expansivities of this silicate system. The results for both beryl and emerald are shown in Fig. 1.

Since there is a change in the sign of the c axis expansion coefficient for beryl at the minimum near 300 °C and hence differences in atomic separations would be minimal and probably indistinguishable, no attempt was made to collect a set of intensity data at a higher temperature for a complete structure determination.

Refinement and results

The positional parameters determined by Belov & Matveeva (1951) were subjected to full-matrix least-squares refinement, using anisotropic thermal parameters. The function $\sum w(F_o - F_c)^2$, was minimized; weights were assigned from counting statistics or set to zero for unobserved reflections when $F_o < F_c$. Structure factors were calculated using Be^{2+}, Al^{3+}, Si^{4+}, and O^{2-} scattering factors from *International Tables for X-ray Crystallography* (1962). An extinction parameter was also included in our least-squares refinement procedure. At this stage of the refinement, the residual $R = \sum||F_o| - |F_c||/\sum|F_o|$ was 0·021. A three-dimensional difference Fourier synthesis calculated at this point contained a broad, positive, low valued peak centered at $0, 0, \frac{1}{4}$, as had been reported by GBM for their hydrous beryl. Therefore, our next step was to include an oxygen atom having a fixed isotropic thermal parameter U of 0·0380 Å^2 (B value of 3·0 Å^2, a typical value found in many hydrates) and also a variable population parameter. Least-squares refinement yielded a population occupancy of 0·0991 (1), corresponding to an approximate composition $Al_2Be_3(SiO_3)_6.0{\cdot}1H_2O$ or $\frac{1}{3}$ of 1 wt.% water. For this refinement, R equaled 0·020. The final positional parameters were in excellent agreement with GBM's values for either anhydrous or hydrous beryl (based on 225 F_{obs}: Gibbs, 1970). It appears that our thermal parameters compare better with GBM's anhydrous beryl values rather than with their hydrous beryl values. In view of the small amount of water present in our crystal specimen, our final

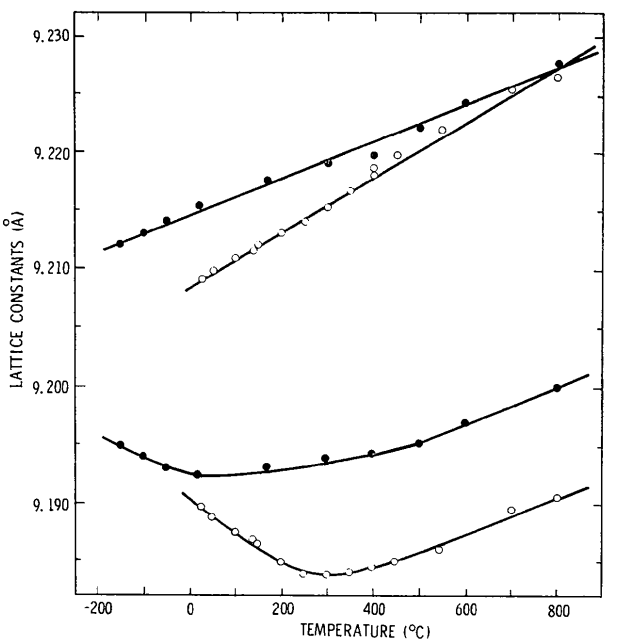

Fig. 1. Lattice constants as a function of temperature for beryl and emerald. The values for the a axis are given at the top, those for the c axis on the bottom. The values for beryl are shown as open circles, while those for emerald appear as solid circles. Note that both crystals exhibit a negative thermal expansion along the c axis. Smooth curves have been drawn through the points for the c axes, and straight lines were drawn through the points for the a axes.

Table 1. *Atomic positional and thermal parameters for beryl*

All values of the thermal parameters are $\times 10^{-2}$ and of the form: $\exp(-2\pi^2 \sum\sum U_{ij}h_ih_ja_i^*a_j^*)$.

	x	y	z	U or U_{11}	U_{22}	U_{33}	U_{12}	U_{13}	U_{23}
Si	0·38749 (2) [0·3875 (2)]	0·11584 (2) [0·1159 (2)]	0	0·343 (5) [0·27 (3)]	0·297 (5)	0·317 (5)	0·162 (4)		
Be	$\frac{1}{2}$	0	$\frac{1}{4}$	0·59 (1) [0·34 (1)]					
Al	$\frac{2}{3}$	$\frac{1}{3}$	$\frac{1}{4}$	0·374 (6) [0·38 (4)]		0·386 (9)			
O(1)	0·31001 (7) [0·3109 (4)]	0·23661 (7) [0·2375 (5)]	0	1·01 (1) [0·70 (7)]	0·71 (1)	1·17 (2)	0·66 (1)		
O(2)	0·49884 (4) [0·4992 (3)]	0·14551 (4) [0·1462 (3)]	0·14529 (3) [0·1450 (3)]	0·710 (8) [0·47 (5)]	0·530 (8)	0·525 (7)	0·297 (7)	0·229 (7)	0·051 (6)
O(3)	0	0	$\frac{1}{4}$	3·80*					

* Population parameter for O(3) is 0·0991 (1).

Table 2. *Observed and calculated structure factors for beryl*

Asterisks denote unobserved reflections; F_o and F_c are both $\times 10$.

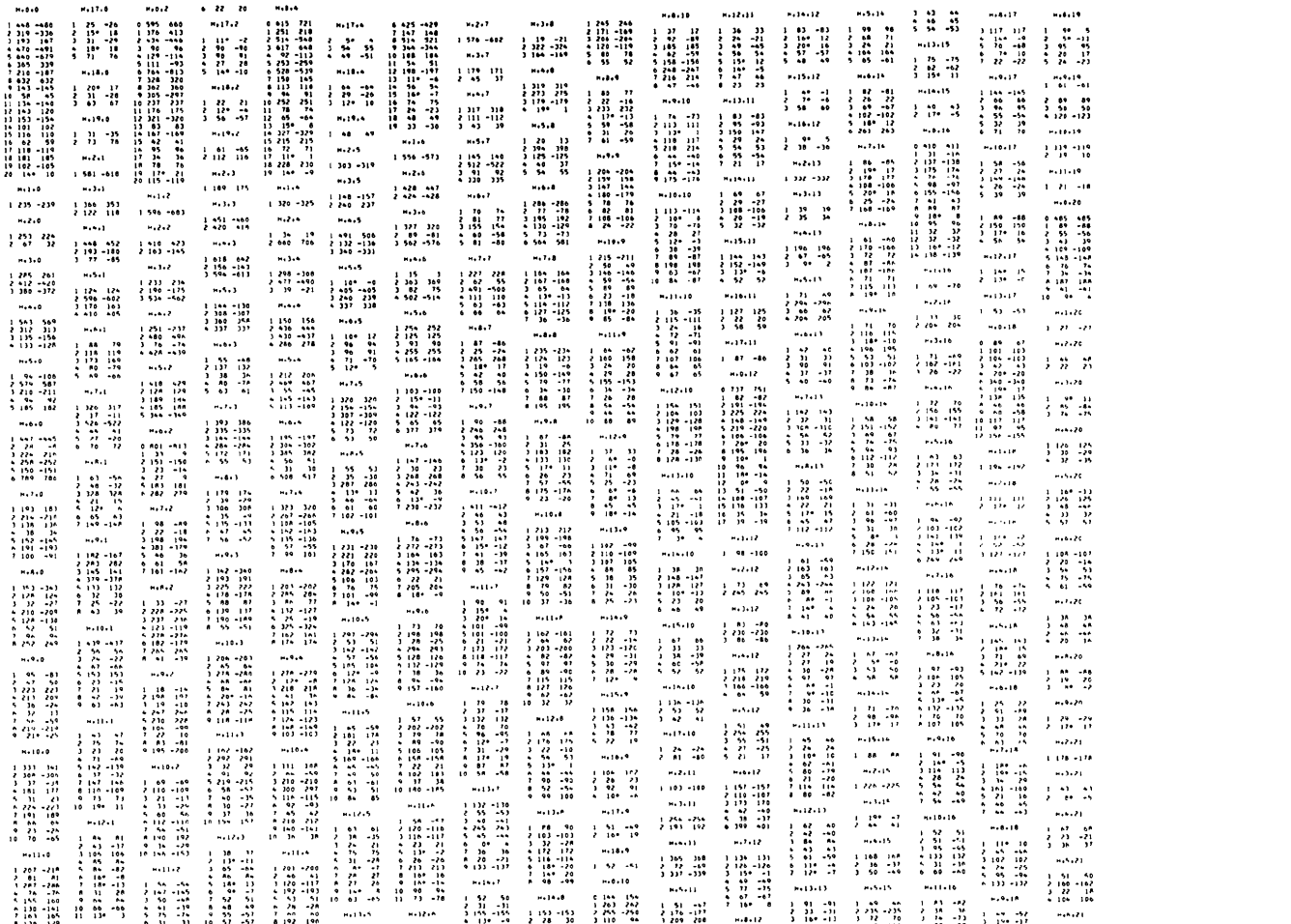

positional and thermal parameters are compared with those of anhydrous beryl in Table 1. The observed and calculated structure factors obtained with these parameters are given in Table 2.

The structure of beryl consists of SiO_4 tetrahedra, which are connected by sharing an oxygen atom of the type O(1) so as to form a ring (Fig. 2). The rings of silica tetrahedra are fused together by bonding,

through oxygen atoms of the type O(2), to Be and Al ions, linking rings located about the $z=0$ and $\frac{1}{2}$ planes. As expected from bonding considerations, the thermal ellipsoids obtained from the anisotropic thermal parameters for O(1) can be approximated by a flattened spheroid. The smallest root-mean-square (r.m.s.) axis (0·084 Å) is normal to the plane bisecting the two Si–O bonds, while the largest r.m.s. axis (0·127 Å) lies in this plane and is perpendicular to the *c* axis. The remaining axis (0·108 Å) lies along the *c* axis. For O(2), the largest r.m.s. axis (0·092 Å) lies almost normal to the plane defined by the atoms to which it is bonded (Si at $z=0$, Be and Al at $z=\frac{1}{4}$; see Fig. 2); of the two other axes (0·066 and 0·074 Å) lying in the plane, the smaller one is essentially along the Si–O bond. Our values for the interatomic separations and angles are listed in Table 3.

Table 3. *Interatomic separations and angles*

(*a*) Involving SiO_4 tetrahedra			
Si—O(1)	1·592 (1) Å	O(1)–Si—O(1^{i})	108·24 (3)°
Si—O(1^{i})	1·594 (1)	O(2)–Si—O(1^{i})	108·42 (2)
Si—O(2)	1·620 (1)	O(2)–Si—O(1)	110·40 (2)
O(1)–O(1^{i})	2·582 (1)	O(2)–Si—O(2^{ii})	110·88 (2)
O(2)–O(1)	2·607 (1)	Si—O(1)–Si	168·24 (3)
O(2)–O(1)	2·638 (1)		
O(2)–O(2)	2·668 (1)		
(*b*) Involving BeO_4 tetrahedra			
Be—O(2)	1·653 (1)	O(2)—Be–O(2^{iii})	90·90 (2)
O(2)—O(2^{iii})	2·355 (1)	O(2)—Be–O(2^{iv})	131·40 (2)
O(2^{iii})–O(2^{iv})	2·688 (1)	O(2^{iii})–Be–O(2^{iv})	108·85 (2)
O(2)—O(2^{iv})	3·012 (1)		
(*c*) Involving AlO_6 octahedra			
Al—O(2)	1·904 (1)	O(2)—Al–O(2^{iii})	76·40 (1)
O(2)–O(2^{iii})	2·355 (1)	O(2)—Al–O(2^{vi})	90·79 (1)
O(2)–O(2^{v})	2·712 (1)	O(2)—Al–O(2^{vii})	96·76 (1)
O(2)–O(2^{vii})	2·847 (1)	O(2^{vii})–Al–O(2^{vi})	170·40 (1)
(*d*) Others			
O(1)–O(2^{vi})	3·124 (1)	Al–O(2)–Be	96·35 (2)
		Al–O(2)–Si	136·57 (2)
		Si–O(2)–Be	127·04 (2)

i.	$+y,\ y-x,\ -z$	I
ii.	$x,\ y,\ -z$	
iii.	$x+y,\ y,\ \frac{1}{2}-z$	
vi.	$1-x-y,\ -y,\ \frac{1}{2}-z$	
v.	$1-x,\ -y,\ z$	
vi.	$x,\ 1-x-y,\ \frac{1}{2}-z$	
vii.	$1-y,\ x-y,\ z$	

Note that the Be and Al environments depart from regularity, the condition required for thermal expansion anisotropy. One can see from the structure that an expansion along the *a* axis, with the rings fixed rigidly and not enlarging, would increase the shorter O(2)–O(2) separation (2·355 Å) at the expense of the longer O(2)–O(2) separation (2·847 Å) about the Al octahedron. Further, rotation (clockwise) of the rings so as to shorten the longer O(2)–O(2) separation (3.012 Å) about the Be tetrahedron, together with an *a* axis expansion, would also result in lengthening the 2·355 Å separation. On the other hand, counterclockwise rotation (with an *a* axis expansion) would lengthen the 3·012 Å separation while maintaining a nearly constant 2·847 Å separation, with the 2·355 Å separation slightly lengthening. If the latter motion is coupled with a slight *c* axis contraction, the lengthened directions diminish. It was not possible to experimentally determine which of these hypothesized movements indeed occurs (by another full-structure determination at higher temperature), because the length of the *c* axis decreases by only about one part in a thousand before normal positive expansion resumes. The expected change in the position parameters at high temperature is, therefore, of the same order of magnitude as our errors in this highly overdetermined structure; hence, it cannot be detected.

The thermal expansion behavior of beryl and emerald can best be compared by considering the lattice constants over a large temperature range. Otherwise, the values of the linear expansivities at a particular temperature, such as room temperature, appear to be in gross disagreement. As Fig. 1 illustrates, the *a* axes for beryl and emerald expand in a linear fashion with linear expansivities of $+(2{\cdot}6\pm0{\cdot}1)\times10^{-6}\,°C^{-1}$ and $+(1{\cdot}7\pm0{\cdot}1)\times10^{-6}\,°C^{-1}$ respectively. The linear expansivities along the *c* axes, however, change signs. For beryl near room temperature, the *c* axis expansivity decreases from a value of $-(2{\cdot}9\pm0{\cdot}4)\times10^{-6}\,°C^{-1}$ to zero near 300 °C and then increases and attains a value of $+(1{\cdot}7\pm0{\cdot}2)\times10^{-6}\,°C^{-1}$ in the region above 400 °C. For emerald, an initial measured value along the *c* axis of $-(2{\cdot}2\pm0{\cdot}4)\times10^{-6}\,°C^{-1}$ decreases, reverses sign near ~100 °C and then attains a higher temperature value at 500 °C of $+(1{\cdot}7\pm0{\cdot}2)\times10^{-6}\,°C^{-1}$. One must use care in comparing these *c* axis expansivities

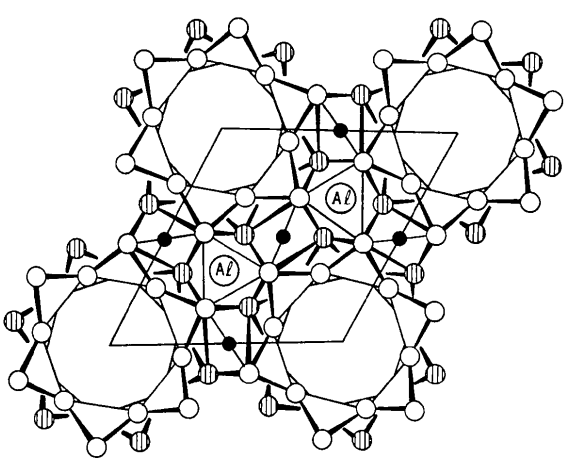

Fig. 2. A schematic representing the structure of beryl viewed along the *c* axis. The medium sized circles are oxygen atoms, small solid circles are beryllium ions, and the larger labeled circles are aluminum ions. Silicon atoms, located in the center of tetrahedra of oxygen atoms, are not shown. These SiO_4 tetrahedra are connected by sharing an oxygen atom so as to form rings, one each about $z=0$ (shown as open oxygen atoms) and about $z=\frac{1}{2}$ (shown as shaded oxygen atoms.

with other literature values, because different impurity levels of the crystal specimen examined may shift the minimum in the *c* axis *vs.* temperature curve. For example, Erfling (1939) found a *c* axis expansivity value for beryl that, at about 100°C, was $-2{\cdot}0\times 10^{-6}°C^{-1}$ and which decreased to $-1{\cdot}43\times 10^{-6}°C^{-1}$ at room temperature, while the expansivity along the *a* axis changed from $-0{\cdot}52\times 10^{-6}°C^{-1}$ at −200°C to $+1{\cdot}05\times 10^{-6}°C^{-1}$ at room temperature. Room-temperature values for emerald from the *Handbook of Chemistry and Physics* (1957) are $1{\cdot}00\times 10^{-6}°C^{-1}$ and $-1{\cdot}35\times 10^{-6}°C^{-1}$ for *a* axis and *c* axis expansivities; these compare better with Erfling's beryl values than with the present values of either beryl or emerald, and suggest the importance of impurities in affecting the thermal expansion behavior of this silicate system.

Returning to the question of atomic movements, it is known that the lattice constants for beryl and emerald can be determined with a greater precision than the atomic locations, and these constants appear to corroborate the above mentioned hypothesis on the movement of the silicate rings with temperature. Note that the lattice constants for beryl and emerald at room temperature differ by $\sim 5\times 10^{-4}$ Å, and that the radii of Al^{3+} and Cr^{3+} can be taken as 0·61 and 0·70 Å respectively (Shannon & Prewitt, 1969). Further, an Al^{3+} ion constitutes about 15% of a linear dimension in the cell, while the difference of the radii is about 15% with a concentration dopant level of Cr ions of about 3%; this suggests a difference $(0{\cdot}15\times 0{\cdot}15\times 0{\cdot}03\simeq 6\times 10^{-4})$ in the lattice constants of beryl and emerald can be expected, and is found to be of the same order of magnitude as that observed. The introduction of Cr^{3+} ions into the beryl structure results in a corresponding expansion of the lattice, as indicated in the above mentioned hypothesis, *i.e.* the rings are moved away from each other to accommodate the larger Cr^{3+} radius. This implies that the thermal expansion behavior of emerald may be similar to beryl, but with a shift on the temperature scale. Indeed, the minimum on the *c* axis expansivity is shifted in temperature some 200°. The added lengthening on the Be–O separations (as well as the Al–O separations, which are also lengthened) probably tend to resist the rotation of the rings, yielding a shallower minimum in the *c* axis *vs.* temperature curve for emerald than for beryl.

Discussions and suggestions by Dr R. W. Lynch, and technical assistance on data collection by Mr R. A. Trudo, are gratefully acknowledged.

References

BELOV, N. V. & MATVEEVA, R. G. (1951). *Doklady Akad. Nauk SSSR*, **6**, 69.

BRAGG, W. L. & WEST, J. (1926). *Proc. Roy. Soc.* p. 691.

CARTZ, L. (1968). In *Anisotropy in Single-Crystal Refractory Compounds*. Vol. 1, pp. 383-389. Eds. F. W. VAHLDICK & S. A. MERSOL. New York: Plenum Press.

ERFLING, H. D. (1939). *Ann. Phys.* **34**, 136.

GIBBS, G. V. (1970). Private communication.

GIBBS, G. V., BRECK, D. W. & MEAGHER, E. P. (1968). *Lithos*, **1**, 275.

Handbook of Chemistry and Physics (1957). 38th ed., p. 1060. Cleveland: Chemical Rubber Publishing Co.

International Tables for X-ray Crystallography (1962). Table 3.3.1*A*, Vol. III. Birmingham: Kynoch Press.

LI, C. T. & PEACOR, D. R. (1968). *Z. Kristallogr.* **126**, 46.

LYNCH, R. W. & MOROSIN, B. (1971). *J. Appl. Cryst.* **4**, 352.

MOROSIN, B. & LYNCH, R. W. (1971). Amer. Cryst. Assoc., South Carolina Meeting, F6.

SHANNON, R. D. & PREWITT, C. T. (1969). *Acta Cryst.* B**25**, 925.

Acta Cryst. (1972). B**28**, 1903

The Crystal Structure of Ammonium Sulphamate

BY V. K. WADHAWAN AND V. M. PADMANABHAN

Nuclear Physics Division, Bhabha Atomic Research Centre, Trombay, Bombay 85 (*AS*), *India*

(*Received* 9 *June* 1971 *and in revised form* 11 *October* 1971)

Ammonium sulphamate, $NH_4NH_2SO_3$, crystallizes in the orthorhombic space group *Pbca*, with eight formula units in a unit cell of dimensions $a=7{\cdot}558$ (6), $b=7{\cdot}835$ (9), and $c=14{\cdot}49$ (2) Å. The crystal structure has been determined by the symbolic addition method and refined by full-matrix least squares to an *R* value of 0·095. The sulphamate tetrahedron is slightly distorted, the S–O distances being 1·45 (1), 1·46 (1) and 1·49 (1) Å. The S–N bond distance is 1·63 (1) Å, which is in between single and double bond values, indicating $(p\rightarrow d)$ π-bonding. The sulphamate and ammonium ions are arranged in columns parallel to the **a** and **c** directions and are held together by a network of hydrogen bonds.

Introduction

A neutron-diffraction study of potassium sulphamate, KNH_2SO_3, by Cox, Sabine, Padmanabhan, Ban, Chuang & Surjadi (1967) indicated that the nitrogen atom is tetrahedrally surrounded by one sulphur and two hydrogen atoms, with a lone pair of electrons in the fourth tetrahedral direction. The N–S bond length